Inorganic Chemistry

Article

pubs.acs.org/IC

Synthesis, Structure, and Magnetic and Electrochemical Properties of Quasi-Linear and Linear Iron(I), Cobalt(I), and Nickel(I) Amido Complexes

Chun-Yi Lin,[†] James C. Fettinger,[†] Fernande Grandjean,[‡] Gary J. Long,*[,‡] and Philip P. Power*[,†]

[†]Department of Chemistry, University of California, One Shields Avenue, Davis, California 95616, United States

[‡]Department of Chemistry, Missouri University of Science and Technology, University of Missouri, 1870 Miner Circle, Rolla, Missouri 65409-0010, United States

Supporting Information

ABSTRACT: Three potassium crown ether salts, $[K(Et_2O)_2(18\text{-crown-6})][Fe\{N(SiMe_3)Dipp\}_2]$ (**1a**; Dipp = C_6H_3-2,6-Pr^i_2), $[K(18\text{-crown-6})][Fe\{N(SiMe_3)Dipp\}_2]\cdot 0.5PhMe$ (**1b**), and $[K(18\text{-crown-6})][M\{N(SiMe_3)Dipp\}_2]$ (M = Co, **2**; M = Ni, **3**), of the two-coordinate linear or near-linear bis-amido monoanions $[M\{N(SiMe_3)Dipp\}_2]^-$ (M = Fe, Co, Ni) were synthesized by one-electron reduction of the neutral precursors $M\{N(SiMe_3)Dipp\}_2$ with KC_8 in the presence of 18-crown-6. They were characterized by X-ray crystallography, UV−vis spectroscopy, cyclic voltammetry, and magnetic measurements. The anions feature lengthened M−N bonds in comparison with their neutral precursors, with slightly bent coordination (N−Fe−N = ca. 172°) for the iron(I) complex, but linear coordination for the cobalt(I) and nickel(I) complexes. Fits of the temperature dependence of $\chi_M T$ of **1** and **2** reveal that the iron(I) and cobalt(I) complexes have large negative D zero-field splittings and a substantial orbital contribution to their magnetic moments with L = 2, whereas the nickel(I) complex has at most a small orbital contribution to its magnetic moment. The magnetic results have been used to propose an ordering of the 3d orbitals in each of the complexes.

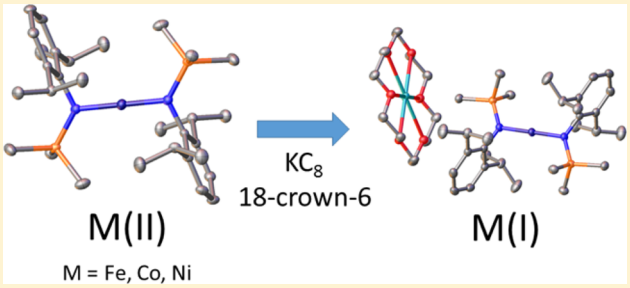

INTRODUCTION

Two-coordinate, open-shell (d^1−d^9) transition-metal complexes are of increasing interest because of their potential applications in areas such as small-molecule activation, catalysis, and single-molecule magnetism.[1] Nonetheless, they remain one of the less well-known series of transition-metal complexes because of the difficulties in stabilizing the low coordination and preventing association or decomposition. They generally are very air and moisture sensitive and display high reactivity due to their coordinative unsaturation. Most two-coordinate, open-shell complexes have bent geometries and are generally difficult to obtain with strictly linear coordination, a geometry which is of particular importance for their magnetic behavior.[1a,e−h] Most feature the metal in the +2 oxidation state, although +1 complexes are becoming more common. Examples of the latter include quintuply bonded dichromium(I) species[2] ArCrCrAr (Ar = $Ar^{Pr^i_4}$ = C_6H_3-2,6(C_6H_3-2,6-Pr^i_2)$_2$, $Ar^{Pr^i_4}$-4-X, X = $SiMe_3$, OMe, F) and the heteroleptic Cr(I) complexes[3] $Ar^{Pr^i_8}CrL$ ($Ar^{Pr^i_8}$ = C_6H-2,6-(C_6H_2-2,4,6-Pr^i_3)$_2$-3,5-Pr^i_2, L = THF, PMe_3). Hillhouse,[4] Tatsumi,[5] and co-workers showed that sterically demanding N-heterocyclic carbenes could stabilize two-coordinate Ni(I) amido or thiolato derivatives.

The use of neutral bulky N-heterocyclic carbenes or the cyclic alkyl(amino)carbene ligands has allowed the isolation of two-coordinate homoleptic Mn(I),[6] Co(I),[7] Ni(0), and Ni(I)[8] complexes. An almost-linear iron(I) dialkyl anion[1e] was obtained by Long and co-workers[9] by one-electron reduction of $Fe\{C(SiMe_3)_3\}_2$. Tilley and co-workers[1c] reduced $Ni\{N(SiMe_3)Dipp\}_2$ (Dipp = C_6H_3-2,6-Pr^i_2) with KC_8 and subsequently exchanged K^+ ion with NBu_4^+ cation to obtain the corresponding Ni(I) salt, whose chemistry was explored.[10] In a previous report we showed that the amido ligand $-N(SiMe_3)Dipp$ could stabilize a series of neutral two-coordinate M^{2+} transition-metal complexes that had a structure in which the ligands had an eclipsed conformation consistent with the presence of dispersion forces.[1a,11]

Herein we report the synthesis and characterization of a series of two-coordinate metal(I) amido complexes $[K(18\text{-crown-6})][M\{N(SiMe_3)Dipp\}_2]$ (M = Fe (**1**·0.5PhMe, i.e. **1b**), Co (**2**), Ni (**3**)) and the ether-complexed species $[K(Et_2O)_2(18\text{-crown-6})][Fe\{N(SiMe_3)Dipp\}_2]$ (**1a**).

Received: June 28, 2014
Published: August 13, 2014

   dx.doi.org/10.1021/ic501534f | Inorg. Chem. 2014, 53, 9400−9406

Scheme 1. Synthesis of 1−3

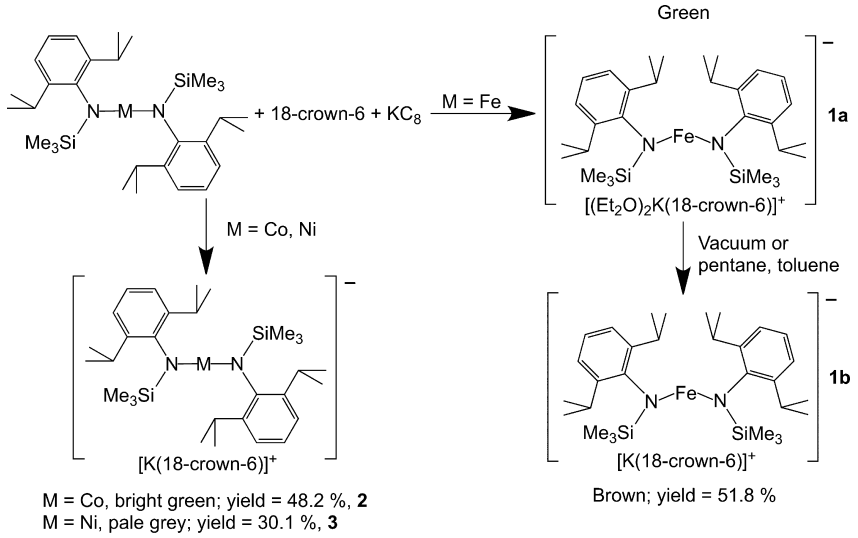

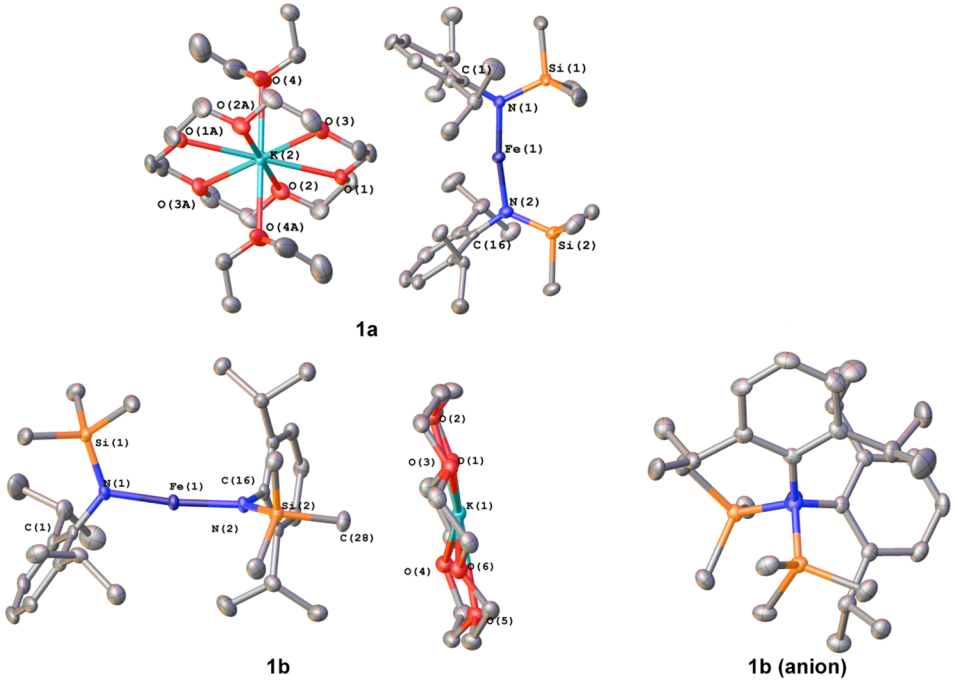

Figure 1. (top) The molecular structure of the cation (left) and the anion (right) of **1a**. H atoms and the disordered component are not shown for clarity. (bottom left) The molecular structure of **1b** (i.e., **1**·0.5PhMe). H atoms and cocrystallized toluene molecule are not shown for clarity. (bottom right) Axial view of **1b** illustrating the almost 90° dihedral angle. Thermal ellipsoids are shown at 30% probability.

RESULTS AND DISCUSSION

Syntheses and Structures. Reduction of the complexes $M\{N(SiMe_3)Dipp\}_2$ (M = Fe, Co, Ni) by KC_8 in the presence of 18-crown-6 in Et_2O proceeded smoothly and produced crystalline products which were identified as the salts $[K(18\text{-crown-6})][M\{N(SiMe_3)Dipp\}_2]$ by single-crystal X-ray crystallography (see Scheme 1).

In the reduction of $Fe\{N(SiMe_3)Dipp\}_2$, green crystals of **1a** formed from Et_2O solution below ca. −18 °C, X-ray crystallography showed that, in addition to an 18-crown-6 ligand, two Et_2O molecules are coordinated to the potassium cation (Figure 1; selected structural parameters are given in Table 1). A comparison of the structure of $Fe\{N(SiMe_3)Dipp\}_2$ and the $[Fe\{N(SiMe_3)Dipp\}_2]^-$ anion of **1a** showed significant differences. In **1a**, the iron(I) has a bent coordination (N−Fe−N angle 171.99(6)°) and has longer Fe−N distances of 1.9127(14) and 1.9176(14) Å, in comparison with the 1.8532(13) Å observed in $Fe\{N(SiMe_3)Dipp\}_2$.[1,11] In addition, whereas $Fe\{N(SiMe_3)Dipp\}_2$ displayed a planar eclipsed $M\{NSiC(ipso)\}_2$ core array, in **1a** the two NSiC(ipso) planes have a dihedral angle of 20.13(10)°, with two Dipp substituents *Z* with respect to each other rather than the *E* conformation in the neutral complex.

The green crystals lost Et_2O upon standing, under reduced pressure, or on dissolution in noncoordinating solvents such as pentane or toluene to form the brown **1**, $[K(18\text{-crown-6})][Fe\{N(SiMe_3)Dipp\}_2]$ (Scheme 1), whose structure (as **1**·0.5PhMe; i.e. **1b**) was also determined by X-ray crystallography.

dx.doi.org/10.1021/ic501534f | Inorg. Chem. 2014, 53, 9400−9406

Table 1. Selected Interatomic Distances (Å) and Angles (deg) for Compounds 1a,b, 2, and 3

	1a	1b	2	3
M(1)–N(1)	1.9127(14)	1.9135(14)	1.8835(10)	1.8493(9)
M(1)–N(2)	1.9176(14)	1.9147(14)		
N(1)–Si(1)	1.7042(15)	1.7136(15)	1.7000(10)	1.7039(9)
M(1)···C(1)	2.922(2)	2.830(2)	2.801(1)	2.781(1)
K(1)···H_{Me} approach		2.91(2)	3.00(2), 3.060(18)	2.960(17), 3.078(16)
N(1)–M(1)–N(2)	171.99(6)	172.65(6)	180	180
M(1)–N(1)–C(1)	115.15(7)	118.94(11)	115.54(7)	116.38(7)
M(1)–N(1)–Si(1)	121.89(11)	117.39(8)	117.90(6)	116.87(5)
C(1)–N(1)–Si(1)	122.96(11)	123.66(11)	125.83(8)	126.15(7)

In the anion the N–Fe–N angle increases slightly to 172.65(6)° and the Fe–N distances of 1.9135(14) and 1.9147(14) Å remain essentially unchanged from those of **1a**. In **1b** the two NSiC(ipso) planes have a dihedral angle of 89.47(6)°, similar to that observed between the NC_2 planes in the structure of Fe{N(Bu^t)$_2$}$_2$, which has a dihedral angle of 80.5(1)°.[12] The increased Fe–N bond distances in the anions of **1a,b** can be explained on the basis of the decreased electrostatic attraction between the Fe(I) ion and the ligands and the overall negative charge of the anion. Although the Fe–N distances in **1a,b** are longer than that in Fe{N(SiMe$_3$)-Dipp}$_2$, they fall within the known range of Fe–N single-bond lengths of 1.842(2)–1.938(2) Å in two-coordinate Fe(II) complexes[1] and are shorter than some Fe–N distances in neutral complexes, such as Fe{N(SiMe$_2$Ph)$_2$}$_2$[13] with Fe–N_{avg} = 1.916(2) Å and Fe{N(Mes)B(Mes)$_2$}$_2$[14] with Fe–N_{avg} = 1.938(2) Å. Although **1a,b** deviate from linearity, no short secondary contacts were observed between the iron(I) and the amido ligand substituents. The closest approaches between ligand atoms and iron involve the *ipso* carbon (C(1)) of the aryl ring at distances of 2.922(2) Å (**1a**) and 2.830(2) Å (**1b**). These distances are both longer than the closest approach of 2.686 Å in Fe{N(SiMe$_3$)Dipp}$_2$. Secondary interactions (K···H–C) may exist between the K^+ and the CH_3 group of the SiMe$_3$ substituents, where K···H_{Me} distances of 2.91(2) and 2.91(2) Å and a K···C distance of 3.198(2) Å were observed. Complexes **1a,b** represent the first two-coordinate Fe(I) amido complexes. The closest related species is the Fe(I) dialkyl anion complex [K(crypt-222)][Fe{C(SiMe$_3$)$_3$}$_2$], in which the iron(I) is in an almost linear C–Fe–C coordination with a C–Fe–C angle of 179.2(2)°; however, no significant Fe–C elongation was observed upon reduction, as the average Fe–C distance of 2.060(4) Å in [K(crypt-222)][Fe{C(SiMe$_3$)$_3$}$_2$] does not differ significantly from the 2.054(4) Å distance in [Fe{C(SiMe$_3$)$_3$}$_2$].[1f,g,9]

X-ray data for crystals of **2** and **3** showed that they are isomorphous and they have very similar cell parameters; see the Supporting Information. Like their M(II) congeners, the anions have linear N–M–N coordination with a center of symmetry located at the metal ion and have a planar eclipsed M{NSiC(ipso)}$_2$ structure similar to that in their neutral congeners (Figure 2). The Co–N bond of 1.8835(10) Å is ca. 0.066 Å longer than the Co^{II}–N bond of 1.8180(14) Å in Co{N(SiMe$_3$)Dipp}$_2$.

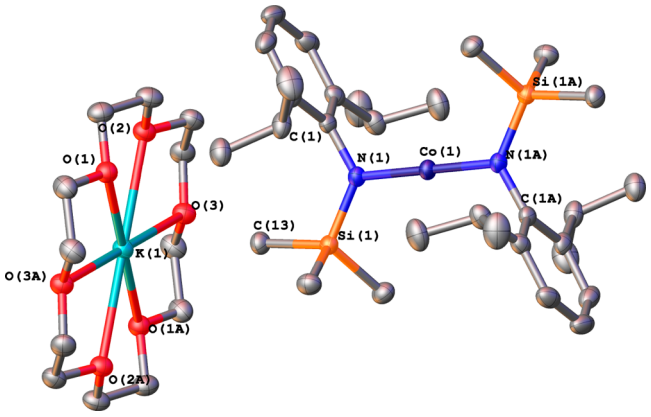

Figure 2. Molecular structure of **2**. The H atoms are not shown for clarity, and the thermal ellipsoids are shown at 30% probability.

The Ni^I–N bond length in **3** is 1.8493(9) Å and is about 0.046 Å longer than the length of 1.8029(9) Å in its neutral precursor. The distance is similar to those in the two-coordinate Ni(I) amido carbene complexes (IPr)Ni{N(SiMe$_3$)$_2$}[4] (Ni–N = 1.865(2) Å; IPr = {CHN(Dipp)}$_2$C), (IPr)NiN(H)Dipp[4] (Ni–N = 1.831(4) Å), and (IPr)NiN(SiMe$_3$)Dipp[8b] (Ni–N = 1.8271(14) Å) and the Ni–N distances of 1.8437(17) and 1.8516(17) Å in [NBu$_4$][Ni{N(SiMe$_3$)Dipp}$_2$],[10] in which the N–Ni–N arrangement is not linear with an angle N–Ni–N of 176.51(8)° and the two aryl groups are cis rather than trans with respect to each other, suggesting that the conformation and the N–M–N angle in the solid state is also cation-dependent. No short nonbonded contacts between metal ions and ligands were observed in **2** and **3**, and the M(1)···C(1) distances are 2.801(1) Å (**2**) and 2.781(1) Å (**3**) and are longer than those in their neutral precursors, which have distances of 2.650(1) Å (**2**) and 2.612(1) Å (**3**). As in the iron(I) analog **1**, close interactions between K^+ and H_{Me} are observed in **2** and **3** with average K···H_{Me} distances of 3.03(2) Å (**2**) and 3.019(17) Å (**3**) and K···C distances of 3.3392(12) Å (**2**) and 3.3432(12) Å (**3**). Although some Ni(I) complexes have been reported recently, complex **3** features the first strictly linear example of N–Ni–N coordination for Ni(I).

Figure 3 provides some further details of the changes that occur in the core structures of **2** and **3** upon reduction. The

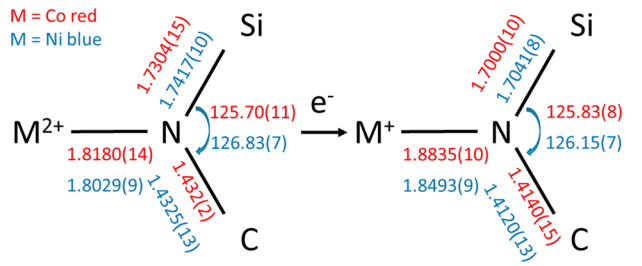

Figure 3. Comparison of the metrical parameters of the M{NSiC(ipso)} bonding of **2** and **3**.

lengthening of the M–N bonds has been discussed above, but the reduction also results in a shortening of the N–C and N–Si bonds. The lower attraction of a metal(I) ion for the nitrogen electron density in comparison to a metal(II) ion increases its attraction for its silyl and Dipp substituents, resulting in shorter N–Si and N–C bonds.

dx.doi.org/10.1021/ic501534f | Inorg. Chem. 2014, 53, 9400–9406

Magnetic Studies. Strictly linear and near-linear two-coordinate, open-shell transition-metal complexes are of interest because of their magnetic properties.[1a,d−f] Previous magnetic studies[1e−h] have reported that two-coordinate linear complexes can exhibit negative D values and slow magnetic relaxation and thus can potentially serve as single-molecule magnets. As will be seen in the following, these reports[1e−h] of properties can be extended from the monoanionic $[Fe\{C(SiMe_3)_3\}_2]^-$ two-coordinate linear complex to the analogous iron(I), cobalt(I), and nickel(I) complexes studied herein.

Magnetic studies yield the $\chi_M T$ results for **1**−**3** shown in Figure 4. The $\chi_M T$ results have been fit between 2 and 300 K by

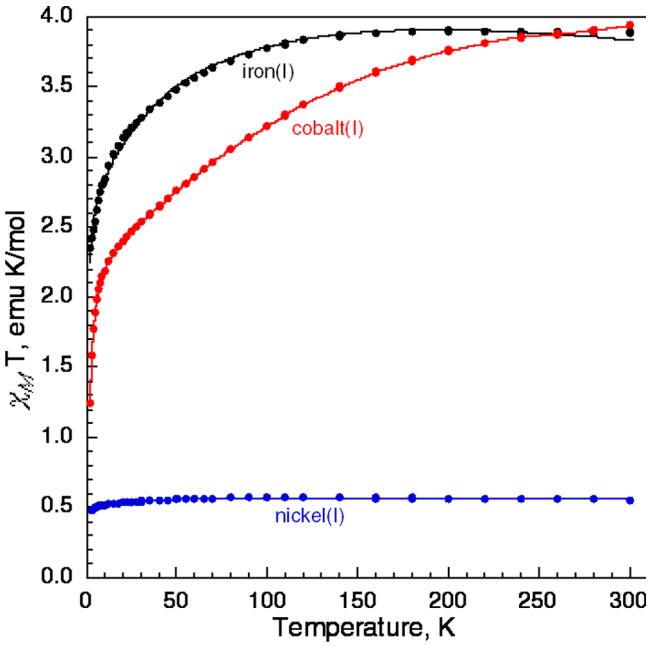

Figure 4. Temperature dependence of $\chi_M T$ for **1** (in black), **2** (in red), and **3** (in blue), obtained upon warming from 2 to 300 K in a 100 Oe applied magnetic field and its fit (solid lines) with the parameters given in the text.

using the PHI code;[15] the resulting fit is shown by the solid lines in Figure 4. For the $3d^7$ iron(I) in **1**, with $S = {}^3/_2$, $L = 2$, and $\lambda = -112$ cm^{-1}, the best fit corresponds to $D = -65(5)$ cm^{-1}, $E = \pm 20(10)$ cm^{-1}, $g_z = 1.85(2)$, $g_x = g_y = 2.11(1)$, and $zJ = -0.047(2)$ cm^{-1}. For the $3d^8$ cobalt(I) in **2**, with $S = 1$, $L = 2$, and $\lambda = -227$ cm^{-1}, the best fit corresponds to $D = -183(10)$ cm^{-1}, $E = \pm 60(5)$ cm^{-1}, $g_z = 2.34(1)$, $g_x = g_y = 3.43(2)$, and $zJ = -0.078(5)$ cm^{-1}. For the $3d^9$ nickel(I) in **3**, with $S = {}^1/_2$ and $L = 0$, the best fit corresponds to $g_z = 2.48(2)$, $g_x = g_y = 2.43(1)$, and $zJ = -0.305(5)$ cm^{-1}. In these fits, χ_M is the molar magnetic susceptibility, while D and E are the axial and rhombic zero field splitting parameters, λ is the spin−orbit coupling constant, g_i are the principal components of the **g** tensor, and zJ is the mean field approximation of any long-range magnetic exchange coupling to χ_M. Although alternate fits are often seemingly reasonable, they lead to fit parameters that are totally unrealistic and/or incompatible with the 5 K magnetization results. The magnetizations of **1**−**3**, obtained at 5 K between 0 and 7 T, and the magnetizations calculated with the above parameters are discussed and shown in Figure S1 in the Supporting Information. Although the fits of $\chi_M T$ shown in Figure 4 are essentially perfect, the calculations of the 5 K magnetization for **1** and **3** shown in Figure S1 are less satisfactory. In contrast, the calculation of the 5 K magnetization for **2** is essentially a perfect fit. The failure to obtain better agreement between the 5 K calculated and observed magnetization for **1** and **3** is a consequence of the texture present in the samples made up from needlelike crystals (see the last picture in the Supporting Information). The magnetization calculation using the PHI[15] code assumes a random powder sample, which is not the case for the needlelike samples of **1** and **3**, which clearly have retained some texture even in the anchored samples studied.

The above fit of $\chi_M T$ for the iron(I) in **1** with $S = {}^3/_2$ and $L = 2$ indicates that the increasing energy ordering of the iron(I) electronic configuration is different from the conventionally accepted configuration[1a] and is consistent with $(d_{z^2})^2(d_{x^2-y^2},d_{xy})^3(d_{xz},d_{yz})^2$, an ordering and configuration that have recently been reported[1f,g] from ab initio calculations on the structurally related linear two-coordinate anionic $[Fe(C(SiMe_3)_3)_2]^-$ complex. The change in the ordering was rationalized on the basis of strong s−d_{z^2} orbital mixing, a result of the low coordination number and weak ligand field. We believe that the ordering in **1** occurs for the same reasons. The above fit of $\chi_M T$ for the nickel(I) in **3** with $S = {}^1/_2$ and $L = 0$ indicates that the nickel(I) electronic configuration is $(d_{x^2-y^2},d_{xy})^4(d_{xz},d_{yz})^4(d_{z^2})^1$, a configuration that has long been considered the conventional[1a] 3d orbital energy ordering for a linear two-coordinate complex. In contrast, the fit of $\chi_M T$ for the cobalt(I) in **2** with $S = 1$ and $L = 2$ is harder to rationalize but is consistent with the $(d_{xz},d_{yz})^4(d_{x^2-y^2},d_{xy})^3(d_{z^2})^1$ configuration. This configuration is quite different from either of the above configurations and may indicate the importance of the nonaxial nature of the crystal field in the compounds under study. It should be noted that fits of $\chi_M T$ for the cobalt(I) in **2** with $S = 1$ and $L = 0$, 1 are totally unacceptable. The reasons why 4s−3d_{z^2} orbital mixing is much weaker or nonexistent in **2** or **3** are unclear.

One might expect parallel behavior between the metal(I) and metal(II) cations with the same number of 3d electrons. Thus, at least some similarity between the magnetic properties of iron(I) in **1b** and those of a linear two-coordinate cobalt(II) complex, both of which have the $3d^7$ electronic configuration could be anticipated. Indeed, this is the case if one compares the magnetic properties of the iron(I) in $[K(18\text{-crown-}6)][Fe\{N(SiMe_3)Dipp\}_2]$ (**1**) shown above with those[11] of cobalt(II) in $Co\{N(SiMe_3)Dipp\}_2$; they both have $S = {}^3/_2$ and $L = 2$ and the increasing energy ordering of the $3d^7$ electrons as given above: i.e., $(d_{z^2})^2(d_{x^2-y^2},d_{xy})^3(d_{xz},d_{yz})^2$. Similarly, the magnetic properties of nickel(I) in $[K(18\text{-crown-}6)][Ni\{N(SiMe_3)Dipp\}_2]$ (**3**), shown above, are comparable with the magnetic properties reported for a variety of copper(II) complexes with the $3d^9$ electronic configuration. In contrast, for some nonobvious reason, there is little similarity between the magnetic properties of cobalt(I) in $[K(18\text{-crown-}6)][Co\{N(SiMe_3)Dipp\}_2]$ (**2**), shown above, with those[11] of nickel(II) in $Ni\{N(SiMe_3)Dipp\}_2$.

Finally, we can discuss the influence of reduction of the metal(II) cation to metal(I) on the magnetic properties. Upon reduction of the iron(II) in $Fe\{N(SiMe_3)Dipp\}_2$, the magnetic properties point to a change in the electronic configuration from the conventional $(d_{x^2-y^2},d_{xy})^3(d_{xz},d_{yz})^2(d_{z^2})^1$ configuration to the calculated[1f,g] $(d_{z^2})^2(d_{x^2-y^2},d_{xy})^3(d_{xz},d_{yz})^2$ configuration, apparently as a result of low coordination number and low iron(I) valence. Upon reduction of $Co^{II}\{N(SiMe_3)Dipp\}_2$, the magnetic properties indicate a change in the electronic

dx.doi.org/10.1021/ic501534f | Inorg. Chem. 2014, 53, 9400−9406

Table 2. Selected Electronic Absorption Spectral Data for 1b, 2, and 3

	wavelength (nm)									
complex										
1b	209	242				428	626		908	1296
2	215	239	284	338	392			758	902	
3	206	239		317						

configuration[11] from the $(d_{z^2})^2(d_{x^2-y^2},d_{xy})^3(d_{xz},d_{yz})^2$ configuration to the unconventional $(d_{xz},d_{yz})^4(d_{x^2-y^2},d_{xy})^3(d_{z^2})^1$ configuration. Finally, upon reduction of the nickel(II) in Ni{N(SiMe$_3$)Dipp}$_2$, the magnetic properties indicate a change in the electronic configuration[11] from $(d_{z^2})^2(d_{x^2-y^2},d_{xy})^4(d_{xz},d_{yz})^2$ to the $(d_{x^2-y^2},d_{xy})^4(d_{xz},d_{yz})^4(d_{z^2})^1$ configuration. In the absence of theoretical calculations, it is difficult to rationalize these changes in electronic configuration, changes that are likely to be related to the unusual geometry around the low-valent metal(I) cation. It is noteworthy that, upon reduction, the iron(I) and cobalt(I) ions keep their large orbital moment of $L = 2$, whereas in the nickel(I) ion the orbital moment is quenched and $L = 0$. An explanation of the quenching of the orbital moment of the linear nickel(II) complex has been based on the proposed existence of π interactions between the nitrogen lone pair p orbitals of the amido ligand and the d_{xz} or d_{yz} orbitals of Ni.[1,16b] However, the reduction of nickel(II) to nickel(I) in **3**, the elongation of the Ni−N bond,[16] and the shortening of the N−Si and N−C bonds (see Figure 2) are consistent with an increase in the electron density at the nitrogen and a weakening of the putative N(L)−Ni π interactions, and hence, perhaps a reduced quenching of the orbital angular momentum, as is reflected in the larger g values for the nickel(I) fit reported above.

Finally, the spin−orbit coupling constants used in the fits[11] of $\chi_M T$ in Fe{N(SiMe$_3$)Dipp}$_2$ and in **1**, on one hand, and in Co{N(SiMe$_3$)Dipp}$_2$ and in **2**, on the other, are close to or constrained to be equal to the free ion values and all four iron(I), iron(II), cobalt(I), and cobalt(II) complexes exhibit very large negative zero-field splitting or crystal field parameters.[11]

Spectroscopy and Electrochemistry. The electronic spectrum of **1b** (see the Supporting Information) in THF displays six absorptions, with the three of longer wavelength having weak intensity tentatively assigned to d−d transitions (nm [ε, M^{-1} cm^{-1}]: 626 [100], 908 [80], 1296 [90]) (Table 2). The other three bands with strong absorptions (nm [ε, M^{-1} cm^{-1}]: 209 [40000], 242 [16000], 428 [4000]) are probably due to the charge transfers from ligand-based N(p) or π orbitals to metal-based d orbitals such as N(p)/aryl $\pi^* \rightarrow d_{z^2}$, N(p)/aryl $\pi^* \rightarrow d_{xz}$, and d_{xz}, $d_{yz} \rightarrow \pi^*$, aryl $\pi \rightarrow d_{xz}$ excitations, as previously shown by calculations for the neutral species M{N(SiMe$_3$)Dipp}$_2$.[11] The experimental spectrum of **2** reveals four strong absorption bands at 215, 239, 284, and 338 nm, possibly from ligand to metal charge transfer, and four weak absorption bands at 392, 758, and 902 nm, probably from d−d transitions. The spectrum of **3** shows three strong absorptions at 206, 239, and 317 nm but no absorption in the longer wavelength region.

Given the interesting reduction properties of the neutral M{N(SiMe$_3$)Dipp}$_2$ complexes which afford **1**−**3**, we performed cyclic voltammetry to further study their redox chemistry. Cyclic voltammetry (see the Supporting Information) of **1** in THF solution revealed two irreversible oxidations that were assigned to Fe(I/II) (E_p = −0.406 V vs Fc/Fc$^+$, Fc = ferrocene) and Fe(II/III) (E_p = 0.250 V vs Fc/Fc$^+$) couples and one irreversible reduction event associated with a Fe(0/I) couple (E_p = −1.886 V vs Fc/Fc$^+$). It should be noted that a reversible Fe(I/II) couple was observed at $E_{1/2}$ = −1.82 V for Fe{C(SiMe$_3$)$_3$}$_2$,[1e] consistent with a more electron donating −C(SiMe$_3$)$_3$ ligand which makes the iron center more electron rich. A cyclic voltammetry study of **2** revealed an irreversible oxidation assigned to Co(I/II) (E_p = −0.152 V vs Fc/Fc$^+$) and a quasi-reversible reduction Co(0/I) (E_p = −1.492 V vs Fc/Fc$^+$) couple. Unlike **1** and **2**, which showed irreversible redox events, **3** revealed a reversible (i_{pa}/i_{pc} = 0.85) Ni(I/II) oxidation event at $E_{1/2}$ =−1.082 V vs Fc/Fc$^+$, which is consistent with the observed[10b] Ni(I/II) reduction couple of Ni{N(SiMe$_3$)Dipp}$_2$ in 1,2-difluorobenzene at $E_{1/2}$ = −1.28 V. However, no reduction couple was observed in the scan range of −0.6 to −2.8 V.

CONCLUSIONS

The use of 18-crown-6 as a complexing agent for K$^+$ has enabled the characterization of the first strictly linear Co(I) and Ni(I) bis-amido complexes. Both structures are very similar to their metal(II) congeners and have elongated M−N bonds. However, the Fe(I) bis-amido complexes [K(Et$_2$O)$_2$(18-crown-6)] [Fe{N(SiMe$_3$)Dipp}$_2$] and [K(18-crown-6)][Fe{N(SiMe$_3$)Dipp}$_2$] do not show linear coordination at the iron(I) ion and exhibit N−Fe−N angles of 171.99(6) and 172.67(7)°, respectively. Magnetic measurements showed that **1** and **2** possess large orbital contribution to their magnetic moments. Work on synthesizing Fe(I) complexes that have strictly linear coordination and exploration of the reaction chemistry of **1b**, **2**, and **3** are currently underway.

EXPERIMENTAL SECTION

All manipulations were performed with the use of modified Schlenk techniques with or in a Vacuum Atmospheres OMNI-Lab drybox. All solvents were dried over an alumina column,[17] followed by storage over a potassium mirror, and were degassed (freeze−pump−thaw) prior to use. 18-crown-6 was purchased from Sigma-Aldrich and used as received. M{N(SiMe$_3$)Dipp}$_2$ (M = Fe, Co, Ni) were prepared according to literature procedures.[11] UV−visible spectra were recorded as dilute THF solutions in 3.5 mL quartz cuvettes with an Olis spectrophotometer. Melting points were measured in glass capillaries sealed under N$_2$ by using a Mel-Temp II apparatus and are uncorrected.

[K(Et$_2$O)$_2$(18-crown-6)][Fe{N(SiMe$_3$)Dipp}$_2$] (1a) and [K(18-crown-6)][Fe{N(SiMe$_3$)Dipp}$_2$]·0.5PhMe (1b). In a Schlenk flask containing freshly prepared KC$_8$ (prepared by heating 0.021 g of K (0.542 mmol) and 0.057 g of graphite (4.77 mmol) until the mixture became a golden color) and a glass-coated magnetic stirring bar was added a Et$_2$O solution of 0.242 g of Fe{N(SiMe$_3$)Dipp}$_2$ (0.438 mmol) and 0.121 g of 18-crown-6 (0.457 mmol) with cooling in an ice bath. After the addition the ice bath was removed and the solution was slowly brought to room temperature and stirred overnight. The orange solution had become dark orange and the solids were allowed to settle. The supernatant liquid was filtered using a filter cannula, and the dark orange filtrate was concentrated to incipient crystallization. Storage at ca. −18 °C overnight afforded large, X-ray-quality bright green crystals

dx.doi.org/10.1021/ic501534f | Inorg. Chem. 2014, 53, 9400−9406

of $[K(Et_2O)_2(18\text{-crown-}6)][Fe\{N(SiMe_3)Dipp\}_2]$ (**1a**). Crystals of **1a** were decanted and dried under vacuum, during which time the green crystals slowly turned brown. They were identified by X-ray crystallography as the compound **1b** (i.e., **1**·0.5PhMe) on crystallization from toluene. Yield: 0.194 g (51.8%). Compound **1b** decomposes and melts as a dark oil at 150−154 °C. UV−vis (THF): λ_{max} (ε_M, M^{-1} cm^{-1}) 209 (40000), 242 (16000), 428 (4000), 626 (100), 908 (80), and 1296 (90) nm.

[K(18-crown-6)][Co{N(SiMe$_3$)Dipp}$_2$] (2). In a Schlenk flask containing freshly prepared KC_8 (prepared by heating 0.015 g of K (0.383 mmol) and 0.048 g of graphite (4.00 mmol) until the mixture turned a golden color) and a glass-coated magnetic stirring bar was added a Et_2O solution of 0.187 g of $Co\{N(SiMe_3)Dipp\}_2$ (0.336 mmol) and 0.0947 g of 18-crown-6 (0.358 mmol) with cooling in an ice bath. After the addition the ice bath was removed and the solution was brought to room temperature and stirred overnight, during which time the dark red solution had become dark green. The salts were allowed to settle, the supernatant solution was filtered using a filter cannula, and the dark green filtrate was concentrated to incipient crystallization. Storage at ca. −18 °C overnight afforded large, X-ray-quality bright yellow-green crystals of $[K(18\text{-crown-}6)][Co\{N(SiMe_3)Dipp\}_2]$. Yield: 0.139 g (48.2%). Anal. Calcd for $C_{42}H_{76}CoKN_2O_6Si_2$: C, 58.7; H, 8.92; N, 3.26. Found: C, 58.3; H, 8.46; N, 3.02. Compound **2** decomposes and melts as a dark oil at 182−184 °C. UV−vis (THF): λ_{max} (ε_M, M^{-1} cm^{-1}) 215 (33000), 239 (18000), 284 (12000), 338 (4900), 392 (4600), 758 (90), and 902 (50) nm.

[K(18-crown-6)][Ni{N(SiMe$_3$)Dipp}$_2$] (3). In a Schlenk flask containing freshly prepared KC_8 (prepared by heating 0.0213 g of K (0.545 mmol) and 0.0723 g of C (6.02 mmol) until the mixture turned a golden color) and a glass-coated magnetic stirring bar was added a Et_2O solution of 0.264 g of $Ni\{N(SiMe_3)Dipp\}_2$ (0.475 mmol) and 0.125 g of 18-crown-6 (0.475 mmol) with cooling in an ice bath. After the addition the ice bath was removed and the solution was slowly brought to room temperature and stirred overnight, during which time the dark purple color of the solution disappeared. The solids were allowed to settle, and the supernatant solution was filtered using a filter cannula. The pale yellow filtrate was concentrated to incipient crystallization, and storage at ca. −18 °C overnight afforded large, X-ray-quality pale yellow crystals of $[K(18\text{-crown-}6)][Ni\{N(SiMe_3)Dipp\}_2]$ (**3**). Yield: 0.123 g (30.1%). Anal. Calcd for $C_{42}H_{76}KN_2NiO_6Si_2$: C, 58.72; H, 8.92; N, 3.26. Found: C, 59.10; H, 8.81; N, 3.01. Compound **3** decomposes and melts as a black oil at 157−161 °C. UV−vis (THF): λ_{max} (ε_M, $M^{-1}cm^{-1}$) 206 (29000), 239 (17000), and 317 (11000) nm.

X-ray Crystallography. Crystals of **1a**,**b**, **2**, and **3** were removed from a Schlenk flask under a stream of nitrogen and immediately covered with a layer of hydrocarbon oil. A suitable crystal was selected, attached to a glass fiber on a copper pin, and quickly placed in the cold N_2 stream on the diffractometer. Data for compounds **1a**,**b** were collected at ca. 90 K on a Bruker APEX II diffractometer with 0.71073 Å Mo Kα radiation. Data for compounds **2** and **3** were collected at 90 K on a Bruker APEX DUO diffractometer with 1.54178 Å Cu Kα_1 and Mo Kα radiation, respectively. Absorption corrections were applied using SADABS.[18] The crystal structures were solved by direct methods and refined by full-matrix least-squares procedures in SHELXTL.[19] All non-H atoms were refined anisotropically. All H atoms were placed at calculated positions and included in the refinement using a riding model. Molecular graphics were produced using the Olex2 program.[20]

Magnetic Measurements. The magnetic measurements have been carried out with a Quantum Design MPMSXL7 superconducting quantum interference magnetometer. The polycrystalline samples of **1**−**3** used for the magnetic measurements were coated with eicosane and sealed under vacuum in a 3 mm diameter, 8 cm length quartz tube with a sample shelf midway down the tube. This sample holder has the advantage that it makes no contribution to the observed magnetic properties. The brown, bright green, and pale yellow colors of **1**−**3**, respectively, were retained throughout the sealing process, and the compounds are stable under vacuum in the sealed quartz tube. For each compound, the sample was zero-field cooled to 2 K and the long moment was measured upon warming to 300 K in an applied field of 100 Oe or 0.01 T. To ensure thermal equilibrium between the powdered sample in the quartz tube and the temperature sensor, the long moment at each temperature was measured until it was essentially constant with time; each set of $\chi_M T$ measurements required ca. 15 h. The magnetization of each sample was subsequently measured at 5 K between 0 and 7 T over a period of 1.25 h. In all cases the sample used was assumed to be free of any solvation and to correspond to the $MC_{42}H_{76}N_2Si_2KO_6$ stoichiometry. The observed long moment has been corrected for the presence of eicosane, which was also used to anchor **1** and **2** in place during the measurements. The observed molar magnetic susceptibility has been corrected for the intrinsic diamagnetic susceptibility by subtracting −0.000618 emu/mol for **1** and −0.000617 emu/mol for **2** and **3**, values that have been obtained from tables of Pascal's constants.[21]

Electrochemistry. Electrochemical measurements were recorded in a glovebox under a N_2 atmosphere using a CH Instruments Electrochemical Analyzer, a glassy-carbon working electrode, a platinum-wire auxiliary electrode, and an $Ag/AgNO_3$ nonaqueous reference electrode. All experiments were performed under a N_2 atmosphere with 0.1 M $Bu^n_4PF_6$ in THF as the electrolyte.

■ ASSOCIATED CONTENT

Ⓢ Supporting Information

Text, figures, tables, and CIFs giving details of syntheses and X-ray crystallography of **1a**,**b**, **2**, and **3**, crystallographic data for **1a**,**b**, **2**, and **3**, magnetization data for **1**−**3** at 5 K, UV−vis−NIR spectra of **1b**, **2**, and **3**, cyclic voltammograms for **1b**, **2**, and **3**, and photographs of crystals of **1a**,**b**, **2**, and **3**. This material is available free of charge via the Internet at http://pubs.acs.org.

■ AUTHOR INFORMATION

Corresponding Authors

*E-mail for G.J.L.: glong@mst.edu.

*E-mail for P.P.P.: pppower@ucdavis.edu.

Notes

The authors declare no competing financial interest.

■ ACKNOWLEDGMENTS

We thank the National Science Foundation (Grant No. CHE-1263760) for support of this work. C.-Y.L. thanks Emily Thompson and Prof. Louise Berben for cyclic voltammetry measurements and Peter Klavins for SQUID magnetic measurements.

■ REFERENCES

(1) For general reviews, see: (a) Power, P. P. *Chem. Rev.* **2012**, *112*, 3482. (b) Kays, D. L. *Dalton Trans.* **2011**, *40*, 769. Examples of catalysis: (c) Lipschutz, M. I.; Tilley, T. D. *Chem. Commun.* **2012**, *48*, 7146. (d) Yang, J.; Tilley, T. D. *Angew. Chem., Int. Ed.* **2010**, *49*, 10186. Examples of single-molecule magnetism for two-coordinate complexes: (e) Zadrozny, J. M.; Atanasov, M.; Bryan, A. M.; Lin, C.-Y.; Rekken, B. D.; Power, P. P.; Neese, F.; Long, J. R. *Chem. Sci.* **2013**, *4*, 125. (f) Zadrozny, J. M.; Xiao, D. J.; Atanasov, M.; Long, G. J.; Grandjean, F.; Neese, F.; Long, J. R. *Nat. Chem.* **2013**, *5*, 577. (g) Zadrozny, J. M.; Xiao, D. J.; Long, J. R.; Atanasov, M.; Neese, F.; Grandjean, F.; Long, G. J. *Inorg. Chem.* **2013**, *52*, 13123−13131. (h) Layfield, R. A. *Organometallics* **2014**, *33*, 1084.

(2) (a) Nguyen, T.; Sutton, A. D.; Brynda, M.; Fettinger, J. C.; Long, G. J.; Power, P. P. *Science* **2005**, *127*, 8545. (b) Wolf, R.; Ni, C.; Nguyen, T.; Brynda, M.; Long, G. J.; Sutton, A. D.; Fischer, R. C.; Fettinger, J. C.; Hellman, M.; Pu, L.; Power, P. P. *Inorg. Chem.* **2007**, *46*, 11277.

(3) Wolf, R.; Brynda, M.; Ni, C.; Long, G. J.; Power, P. P. *J. Am. Chem. Soc.* **2007**, *129*, 6076.

(4) Laskowski, C. A.; Hillhouse, G. L. *J. Am. Chem. Soc.* **2008**, *130*, 13486.
(5) Ito, M.; Matsumoto, K.; Tatsumi, K. *Inorg. Chem.* **2009**, *48*, 2215.
(6) Samuel, P. P.; Mondal, K. C.; Roesky, H. W.; Hermann, M.; Frenking, G.; Demeshko, S.; Meyer, F.; Stuckl, A. C.; Christian, J. H.; Dalal, N. S.; Ungur, L.; Chibotaru, L. F.; Pröpper, K.; Meents, A.; Dittrich, B. *Angew. Chem., Int. Ed.* **2013**, *52*, 11817.
(7) Mo, Z.; Chen, D.; Leng, X.; Deng, L. *Organometallics* **2012**, *31*, 7040.
(8) NHC carbenes−Ni(0): (a) Arduengo, A. J.; Gamper, S. F.; Calabrese, J. C.; Davidson, F. *J. Am. Chem. Soc.* **1994**, *116*, 4391. (b) Caddick, S.; Cloke, F. G. N.; Hitchcock, P. B.; Lewis, A. K.; de, K. *Angew. Chem., Int. Ed.* **2004**, *43*, 5824. (c) Matsubara, K.; Miyazaki, S.; Koga, Y.; Nibu, Y.; Hashimura, T.; Matsumoto, T. *Organometallics* **2008**, *27*, 6020. (d) Danopoulos, A. A.; Pugh, D. *Dalton Trans.* **2008**, 30. (e) Radius, U.; Bickelhaupt, F. M. *Coord. Chem. Rev.* **2009**, *253*, 678. (f) Poulten, R. C.; Page, M. J.; Algarra, A. G.; Le Roy, J. J.; López, I.; Carter, E.; Llobet, A.; Macgregor, S. A.; Mahon, M. F.; Murphy, D. M.; Murugesu, M.; Whittlesey, M. K. *J. Am. Chem. Soc.* **2013**, *135*, 13640. (g) Mondal, K. C.; Samuel, P. P.; Li, Y.; Roesky, H. W.; Roy, S.; Ackermann, L.; Sidhu, N. S.; Sheldrick, G. M.; Carl, E.; Demeshko, S.; De, S.; Parameswaran, P.; Ungur, L.; Chibotaru, L. F.; Andrada, D. M. *Eur. J. Inorg. Chem.* **2014**, 818.
(9) (a) Viefhaus, T.; Schwarz, W.; Hubler, K.; Locke, K.; Weidlein, J. *Z. Anorg. Allg. Chem.* **2001**, *627*, 715. (b) LaPointe, A. M. *Inorg. Chim. Acta* **2003**, *345*, 359. (c) Reiff, W. M.; LaPointe, A. M.; Witten, E. H. *J. Am. Chem. Soc.* **2004**, *126*, 1048.
(10) Lipschutz, M. I.; Yang, X.; Chatterjee, J.; Tilley, T. D. *J. Am. Chem. Soc.* **2013**, *135*, 15298.
(11) Lin, C.-Y.; Guo, J.-D.; Fettinger, J. C.; Nagase, S.; Grandjean, F.; Long, G. J.; Chilton, N. F.; Power, P. P. *Inorg. Chem.* **2013**, *52*, 13584.
(12) Reiff, W. M.; Schulz, C. E.; Whangbo, M. H.; Seo, J. I.; Lee, Y. S.; Potratz, G. R.; Spicer, C. W.; Girolami, G. S. *J. Am. Chem. Soc.* **2009**, *131*, 404.
(13) Chen, H.; Bartlett, R. A.; Dias, H. V. R.; Olmstead, M. M.; Power, P. P. *J. Am. Chem. Soc.* **1989**, *111*, 4338.
(14) Chen, H.; Bartlett, R. A.; Olmstead, M. M.; Power, P. P.; Shoner, S. C. *J. Am. Chem. Soc.* **1990**, *112*, 1048.
(15) Chilton, N. F.; Anderson, R. P.; Turner, L. D.; Soncini, A.; Murray, K. S. *J. Comput. Chem.* **2013**, *34*, 1164.
(16) A number of linear coordinated nickel(II) d^8 complexes are known; they have Ni−N distances of 1.8029(9) Å (Ni{N($SiMe_3$)Dipp}$_2$),[1.1c,11] 1.818(3) Å (Ni{N(H)Ar$^{Pr^i_4}$}$_2$),[16a] and 1.8284(15) Å (Ni{N(H)Ar$^{Pr^i_6}$}$_2$).[16b] (a) Li, J.; Song, H.; Cui, C.; Cheng, J.-P. *Inorg. Chem.* **2008**, *47*, 3468. (b) Bryan, A. M.; Merrill, W. A.; Fettinger, J. C.; Reiff, W. M.; Power, P. P. *Inorg. Chem.* **2012**, *51*, 3366.
(17) Pangborn, A. B.; Giardello, M. A.; Grubbs, R. H.; Rosen, R. K.; Timmens, F. J. *Organometallics* **1996**, *15*, 1518.
(18) *SADABS*, version 5.0; an empirical absorption correction program for the SAINT-Plus-NT; Bruker AXS: Madison, WI, 1998.
(19) *SHELXTL*, version 5.1; Bruker AXS:Madison, WI, 1998.
(20) Dolomanov, O. V.; Bourkis, L. J.; Gilder, R. J.; Howard, J. A. K.; Puschmann, H. *J. Appl. Crystallogr.* **2009**, *42*, 339.
(21) Bain, G. A.; Berry, J. F. *J. Chem. Educ.* **2008**, *85*, 352.

dx.doi.org/10.1021/ic501534f | *Inorg. Chem.* 2014, 53, 9400−9406